Current Biology 22, 2213–2220, December 4, 2012 ©2012 Elsevier Ltd All rights reserved http://dx.doi.org/10.1016/j.cub.2012.09.047

Article

miR-786 Regulation of a Fatty-Acid Elongase Contributes to Rhythmic Calcium-Wave Initiation in *C. elegans*

Benedict J. Kemp,[1] Erik Allman,[2] Lois Immerman,[4] Megan Mohnen,[1] Maureen A. Peters,[4] Keith Nehrke,[3] and Allison L. Abbott[1,*]
[1]Department of Biological Sciences, Marquette University, Milwaukee, WI 53201, USA
[2]Department of Pharmacology and Physiology
[3]Department of Medicine
University of Rochester School of Medicine and Dentistry, Rochester, NY 14642, USA
[4]Department of Biology, Oberlin College, Oberlin, OH 44074, USA

Summary

Background: Rhythmic behaviors are ubiquitous phenomena in animals. In *C. elegans,* defecation is an ultradian rhythmic behavior: every ~50 s a calcium wave initiating in the posterior intestinal cells triggers the defecation motor program that comprises three sequential muscle contractions. Oscillatory calcium signaling is central to the periodicity of defecation. The posteriormost intestinal cells function as the pacemaker for this rhythmic behavior, although it is unclear how the supremacy of these cells for calcium-wave initiation is controlled.

Results: We describe how the loss of the *mir-240/786* microRNA cluster, which results in arrhythmic defecation, causes ectopic intestinal calcium-wave initiation. *mir-240/786* expression in the intestine is restricted to the posterior cells that function as the defecation pacemaker. Genetic data indicate that *mir-240/786* functions upstream of the inositol 1,4,5-trisphosphate (IP_3) receptor. Through rescue analysis, it was determined that miR-786 functions to regulate defecation. Furthermore, we identified *elo-2*, a fatty-acid elongase with a known role in defecation cycling, as a direct target for miR-786. We propose that the regulation of palmitate levels through repression of *elo-2* activity is the likely mechanistic link to defecation.

Conclusions: Together, these data indicate that miR-786 confers pacemaker status on posterior intestinal cells for the control of calcium-wave initiation through the regulation of *elo-2* and, subsequently, palmitate levels. We propose that a difference in fatty-acid composition in the posterior intestinal cells may alter the activities of membrane proteins, such as IP_3-receptor or TRPM channels, that control pacemaker activity in the *C. elegans* intestine.

Introduction

Biological rhythms range from the annual migratory behaviors of animals to the circadian regulation of physiological pathways to the ultradian rhythms of the heart. Many ultradian rhythms, which have cycles of less than a day, are controlled by oscillations of intracellular calcium. Signals from pacemaker cells drive changes in intracellular calcium levels that initiate and coordinate contractions of the heart as well as of smooth muscle tissues, such as the gut [1–4]. Three rhythmic behaviors have been described in *C. elegans*: pharyngeal peristalsis [5], gonadal sheath contractions [6], and defecation [7]. *C. elegans* has been used extensively to study oscillatory calcium signaling and rhythmic behaviors (reviewed in [8]).

The defecation motor program (DMP) is a rhythmic behavior that occurs every ~50 s and comprises three stereotypical contractions: a posterior body-wall muscle contraction, an anterior contraction, and an enteric muscle contraction followed by expulsion. The posterior body-contraction step is initiated by a calcium elevation in the posterior intestine, which requires the inositol 1,4,5-trisphosphate (IP_3)-receptor-mediated release from intracellular calcium stores [9–11] along with an influx of extracellular calcium through the TRPM channels, GON-2 and GTL-1 [12–14]. These calcium elevations lead to the extrusion of protons from the intestine to the pseudocoelomic space via PBO-4/NHX-7 sodium-proton exchanger activity. Pseudocoelomic acidification then triggers the contraction of the posterior body-wall muscle [15, 16].

The posterior intestine functions as the pacemaker in the initiation and coordination of the DMP [7]. The nematode intestine is a single-cell layer tube of 20 polarized epithelial cells that are joined by gap junctions and are organized into nine intestinal rings from the anterior int1 to the posterior int9 [17, 18]. Calcium release in the posterior intestine triggers an anterior-directed intercellular calcium wave throughout the intestine, which is essential for normal execution of the DMP [18, 19]. Hence, cells of the posterior intestinal ring are the site of the behavioral pacemaker [7].

The molecular mechanisms that confer pacemaker activity to the posterior intestine are largely unknown. Pacemaker activity for calcium wave initiation is an intrinsic property of intestinal cells because rhythmic calcium waves persist in isolated intestines [10]. Because all intestinal cells are capable of initiating calcium waves [18, 19], pacemaker activity likely involves establishing a different threshold for intracellular calcium release in the posterior intestine relative to neighboring intestinal cells. Therefore, differences in the expression or activity of critical regulators of calcium sensitivity must exist in the posterior intestine.

microRNAs (miRNAs) are ~22 nt noncoding small RNAs that posttranscriptionally repress translation of downstream target mRNAs [20, 21]. Interestingly, analysis of miRNA deletion mutants identified a miRNA cluster, *mir-240/786*, that functions to regulate defecation cycling. The loss of *mir-240/786* results in long and arrhythmic defecation cycles [22]. Here we show that *mir-240/786* is expressed in the posteriormost int9 cells. We demonstrate that *mir-240/786* mutants display defects in calcium-wave initiation in the posterior intestine. Rescue experiments demonstrate that *mir-786*, not *mir-240*, activity is required for normal defecation cycling. Furthermore, we have identified *elo-2*, which encodes a fatty-acid elongase, previously implicated in defecation behavior [23], as a direct target of miR-786. Our results suggest that miR-786 acts cell autonomously to ensure calcium-wave initiation in the posterior intestinal cells by regulating fatty-acid composition through repression of *elo-2*.

*Correspondence: allison.abbott@marquette.edu

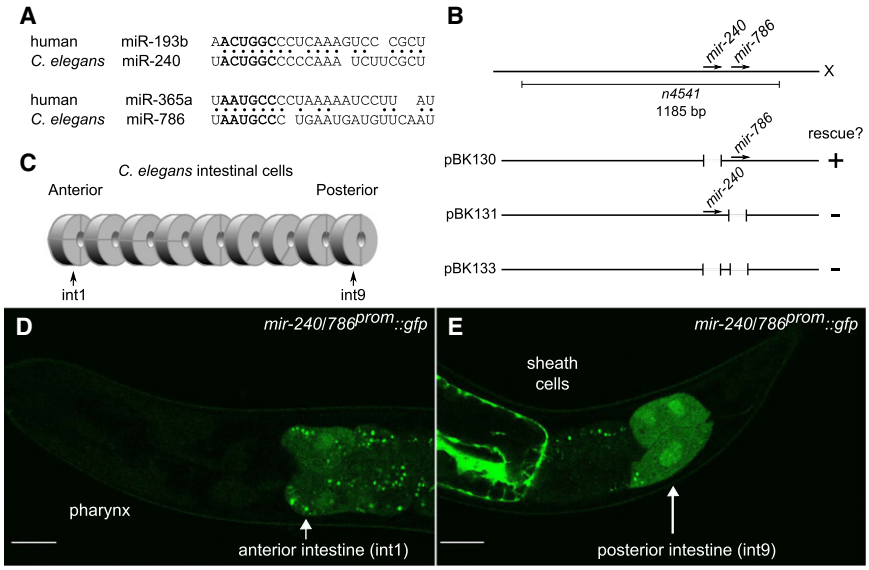

Figure 1. *mir-240/786* Is Expressed in Intestinal Cells

(A) Alignment of miR-193b and miR-365a in humans with miR-240 and miR-786 in *C. elegans*, respectively. Dots indicate bases conserved between humans and *C. elegans*.

(B) The *mir-240* and *mir-786* sequences are separated by only 100 nt on the X chromosome. The deletion, *n4541*, removes 1185 bp. Rescuing activity was observed with a genomic fragment that contains *mir-786*.

(C) Schematic of *C. elegans* intestine with a series of 9 rings of cells from the anterior int1 to the posterior int9, modified from [17].

(D and E) Representative confocal images of the *mir-240/786* promoter driving GFP expression (*mir-240/786*^{prom}*::gfp*). Anterior is to the left. Scale bar represents 20 μm. Weak GFP expression is observed in the int1 anterior ring of cells (D). No expression is observed in the pharynx in adult worms. GFP expression is observed in the posterior int9 cells (E). Expression is also observed in the gonadal sheath cells.

Results

miR-786 Functions to Regulate Defecation

mir-240 and *mir-786* are miRNA genes that are conserved in many species, including humans, where the related miRNA genes are *mir-193b* and *mir-365a*, respectively (Figure 1A). The sequences encoding these two miRNAs are located in a genomic cluster (Figure 1B). We first determined which miRNA in this cluster functions to regulate defection. We performed rescue analysis with genomic fragments that were mutated to delete the 22 nucleotide sequence coding for miR-240, miR-786, or both. Defecation defects were rescued with genomic fragments containing *mir-786* but not *mir-240* (Figure 1, see also Table S1 available online). These results indicate that *mir-786* is necessary for rhythmic defecation cycling in worms.

mir-240/786 Is Expressed in the Intestine and Somatic Gonad

Previously, *mir-240/786* expression was observed in the uterus, spermatheca, and gonadal sheath cells beginning in the L3 stage [24]. Because loss of *mir-240/786* causes defecation arrhythmia [22], we performed further analysis of *mir-240/786* expression to determine whether *mir-240/786* was expressed in cells required for defecation, such as the intestine, body-wall muscle, enteric muscle, or the AVL/DVB neurons [25]. We observed consistent GFP expression in the posteriormost int9 intestinal cells (Figures 1C and 1E) [17]. Weaker expression was observed with lower penetrance in the four cells of the anteriormost int1 intestinal cells (Figure 1D). No expression was observed in the body-wall muscle, enteric muscle, or neurons.

Loss of *mir-240/786* Results in Defects in the Initiation of the DMP

Consistent with earlier observations [22], we found that *mir-240/786* worms display long, arrhythmic defecation cycles, as determined by the length of time between consecutive posterior body-contraction events (Figure 2). Although average defecation-cycle periodicity was consistently longer than in wild-type worms, there was variability in the extent of arrhythmia observed between individual *mir-240/786* mutant worms (Figures 2B and 2C). *mir-240/786* worms displayed additional defects in defecation behavior. First, in contrast to the smooth, rapid posterior contraction in wild-type worms (Movie S1), the posterior contraction in *mir-240/786* mutants often appeared to be biphasic, with an initial weak contraction, followed by a full contraction (Movie S1). This was associated with a longer interval between the posterior contraction and subsequent steps in the motor program: on average, in wild-type worms an expulsion occurred 4.3 ± 0.5 s after a posterior contraction, whereas in *mir-240/786* worms this increased to 5.5 ± 1.9 s. Second, weak posterior contractions that were not associated with a full DMP occurred in 34.6% of the defecation cycles (Movie S1). Finally, *mir-240/786* worms failed to execute an enteric muscle contraction and expulsion following a strong posterior body-contraction event in 14.8% of the cycles (Movie S1).

mir-240/786 Functions Upstream of IP_3-Receptor-Mediated Calcium Release

IP_3-receptor-mediated calcium release in the intestine is an essential regulator of defecation cycling in worms (Figure 3A). The level of IP_3-receptor activity can determine the length of the defecation cycle: worms with reduced activity of *itr-1*, which encodes the IP_3 receptor in worms, display long defecation cycles, whereas worms that overexpress *itr-1*(+) show short defecation cycles [9]. We found the long-defecation phenotype associated with the *itr-1(sa73)* mutant was enhanced in *itr-1(sa73)*; *mir-240/786* double-mutant worms, with some worms failing to show any posterior body contractions during 10 min of monitoring (data not shown).

In order to determine whether *mir-240/786* functioned upstream of *itr-1*, we performed epistasis analysis with gain-of-function alleles of *itr-1*. There are multiple gain-of-function *itr-1* mutations, including the *sy290* allele, which is predicted to enhance IP_3-binding affinity approximately 2-fold [26], and the *sy327* allele, which affects the calcium-binding domain [10]. These mutations have been shown to suppress the long-defecation-cycle phenotypes caused by mutations in upstream signaling processes, such as loss of *plc-3*, which encodes phospholipase Cγ [10]. We found that both the

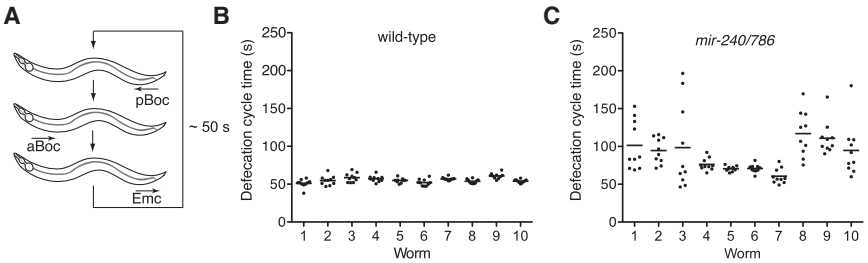

Figure 2. Loss of *mir-240/786* Results in Long, Arrhythmic Defecation Cycles

(A) Diagram of the three contractions of the DMP in *C. elegans*. A posterior body contraction (pBoc) pushes the contents of the intestine toward the anterior. An anterior contraction (aBoc) just behind the pharynx occurs about 3–4 s later that pushes intestinal contents toward the posterior. An enteric muscle contraction (EMC) follows ~1 s later resulting in an expulsion. In wild-type worms, the DMP is executed every ~50 s.

(B and C) Analysis of defecation-cycle time(s) in individual worms. Individual cycle times for each worm are denoted by dots. Ten defecation cycles were analyzed in ten individuals and the mean is listed as a solid line for wild-type worms (B) and *mir-240/786* mutant worms (C).

sy290 and *sy327 itr-1* gain-of-function alleles were able to suppress the defecation defects associated with the loss of *mir-240/786* (Figure 3B).

We next determined whether mutations that result in enhanced levels of IP_3 could also suppress the defecation-cycle defects in *mir-240/786* mutants. Loss of either IP_3 kinase (*lfe-2*) or IP_3 phosphatase (*ipp-5*) activities are expected to result in elevated levels of IP_3, due to reduced conversion of IP_3 into IP_4 or IP_2 (Figure 3A). Like *itr-1* gain-of-function alleles, loss of *lfe-2* or *ipp-5* suppresses defecation defects associated with mutations in upstream signaling processes. We found that loss of *lfe-2* or *ipp-5* was able to suppress the *mir-240/786* defecation defects (Figure 3B). Taken together, these data indicate that *mir-240/786* functions upstream or in parallel to IP_3-receptor activity in the regulation of the DMP.

mir-240/786 Is Necessary for Stereotypical Calcium-Wave Initiation and Confers Pacemaker-Cell Status

Given the central role of the IP_3 receptor in calcium signaling in the *C. elegans* intestine, we next determined how the loss of *mir-240/786* influenced calcium oscillations and calcium-wave propagation during defecation. Live, freely moving animals expressing the calcium biosensor D3cpV [27] in the intestinal cytoplasm were used for dynamic fluorescent imaging to measure the relative change in cytoplasmic calcium throughout the entire intestine in wild-type and *mir-240/786* mutant worms. Representative calcium oscillations are shown in Figures 4A, 4C, and Movie S2. In wild-type worms, each calcium peak represents a fast intercellular calcium wave that initiates in the posterior intestine and propagates anteriorly (Movie S2) [10, 11, 19].

Multiple defects in calcium oscillations were observed in *mir-240/786* mutants. First, calcium oscillations were arrhythmic and differed greatly in magnitude in *mir-240/786* mutants (Figure 4C) relative to wild-type controls (Figure 4A). Second, multiple calcium events occurred in each defecation cycle (Figure 4H), with small calcium increases often preceding successively larger calcium increases, until the DMP was triggered (Figures 4C and S1). Third, the spatial pattern of calcium-wave initiation was strikingly altered in *mir-240/786* mutants. Whereas, in wild-type worms, calcium-wave initiation is restricted to the anterior and posterior ends of the intestine [19], calcium-wave initiation in *mir-240/786* mutants often occurred at ectopic sites in internal intestinal cells (Figure 4G and Movie S2). These ectopic calcium elevations occasionally resulted in both forward and reverse waves (Figures 4E, S1, and Movie S2). However, ectopic calcium waves were often insufficient to elicit a large calcium release in posterior intestinal cells, which is necessary to trigger a posterior body contraction. Thus, in *mir-240/786* mutants, the posterior intestine appears refractory to robust calcium release and wave initiation. Consistent with our behavioral data, we found that the *sy327* gain-of-function allele of *itr-1* was able to fully suppress the arrhythmic calcium oscillations and ectopic calcium-wave initiation associated with loss of *mir-240/786* (Figure S2), suggesting that *mir-240/786* acts upstream of the IP_3 receptor to regulate calcium signaling.

Acidification of the intestinal cytoplasm results from calcium signaling during defecation and contributes to the behavioral output [16]. Consistent with *mir-240/786* acting upstream of the IP_3 receptor, acidification events were arrhythmic in *mir-240/786* worms (Figures 4B and 4D). Individual acidification events looked largely similar to wild-type, although unlike in wild-type worms, low amplitude changes in the cytoplasmic pH in the posterior intestinal cells were observed in *mir-240/786* mutants. These low amplitude pH changes correlated with the observed small calcium elevations and weak posterior contractions (Figures 4F and S1). It is likely that calcium must be elevated over a threshold level to trigger robust acidification and full posterior body contraction. Collectively, these data indicate that *mir-240/786* functions upstream of IP_3-receptor activity to promote calcium elevation and wave initiation in the posterior intestine.

Identification of *elo-2* as a Target of miR-786 in the Posterior Intestine

In order to identify relevant miR-786 targets, we tested computationally predicted targets using RNAi. Typically, miRNAs repress the translation of target mRNAs through imperfect binding to sites in target 3′ UTRs [20]. Thus, the phenotype of *mir-240/786* mutant worms results from elevated levels of miR-786 targets. Candidate targets were identified using mirWIP [28], PITA [29], and Targetscan 5.1 [30, 31]. Of the candidates tested, only knockdown of *elo-2* resulted in a near complete suppression of the long defecation-cycle periodicity in *mir-240/786* worms (Figure 5A and Table S2). *elo-2(RNAi)* also suppressed the weak posterior contractions observed in *mir-240/786* mutants (data not shown). *elo-2* encodes a fatty-acid elongase, which has been shown to regulate defecation cycling [23] and has a single predicted miR-786 binding site in its 3′ UTR (Figure 5B). Knockdown of *elo-2* in wild-type worms alters levels of fatty acids, with a significant increase observed in the level of palmitate (C16:0) [23]. Interestingly, higher levels of *elo-2* specifically in the posterior intestine extended the defecation period [23], similar to the phenotype observed in *mir-240/786* worms.

mir-240/786; elo-2(RNAi) worms had a shorter average-defecation period but still had a higher coefficient of variation (13.8% CV) in the lengths of defecation cycles compared to *elo-2(RNAi)* worms (4.1% CV, Table S2). Calcium imaging of

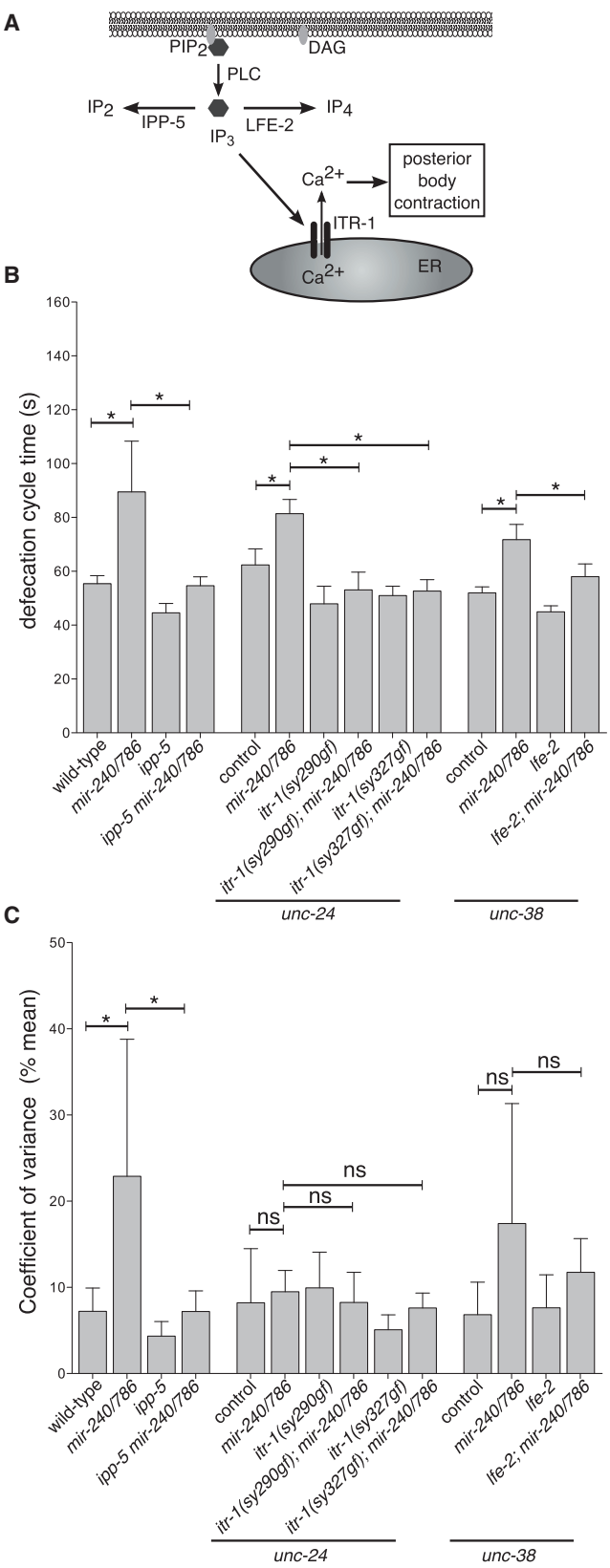

Figure 3. Elevation of IP_3-Receptor Activity Can Suppress *mir-240/786* Defecation Defects

(A) IP_3-mediated pathway for calcium release. Hydrolysis of PIP_2 generates IP_3, which can be converted to IP_4 by the IP_3 kinase, LFE-2, or to IP_2 by the IP_3 phosphatase, IPP-5. IP_3 binds to its receptor, ITR-1, on the endoplasmic reticulum (ER), resulting in the release of intracellular calcium.

(B) Average defecation-cycle times (mean + SD) for wild-type and mutant worms. The average defecation-cycle time was determined by the time between consecutive posterior body contractions (n = 5–10 worms, 10 cycles/worm). Genetic analysis was performed in the *unc-24(e138)* genetic background because available gain-of-function alleles of *itr-1* are linked to this allele. For *lfe-2,* genetic analysis was performed in the *unc-38(x20)* genetic background because the available *lfe-2(sy326)* allele is linked to *unc-38(x20)*.

(C) Variation of cycle time (mean + SD) for wild-type and mutant worms. The average coefficient of variation was calculated for five to ten worms for each strain. *$p < 0.01$. One-way ANOVA and Tukey's test. ns, not significant; $p > 0.05$.

these worms showed that the arrhythmia of calcium oscillations was largely suppressed in *mir-240/786;elo-2(RNAi)*, but surprisingly, knockdown of *elo-2* did not restore calcium-wave initiation to the posterior intestine in *mir-240/786* mutants (Figures 5C and 5D). Instead, these worms showed predominantly anterior-initiated calcium waves, which subsequently triggered a posterior calcium wave and a DMP. This is consistent with the idea that reducing *elo-2* expression amplifies calcium signaling, but the supremacy of the pacemaker is determined by the difference in *elo-2* expression level relative to other cells. Knockdown of *elo-2* in wild-type worms resulted in fast posterior-initiated calcium waves, suggesting that either an *elo-2* gradient persists following knockdown or that there are other mechanisms that help to establish pacemaker supremacy in addition to *elo-2* expression levels.

To test whether *elo-2* is a direct target of miR-786, we first analyzed *elo-2* mRNA levels. A modest increase was observed in *elo-2* mRNA levels in *mir-240/786* worms relative to wild-type worms (Figure S3). In order to determine if *elo-2* is regulated specifically in the posterior intestine, we analyzed the expression of *gfp* under the control of the *elo-2* 5′ promoter and either the *elo-2* 3′ UTR or a mutated *elo-2* 3′ UTR in which the miR-786 putative binding site was deleted. An *elo-2*^{prom}*::gfp* reporter under the control of the *unc-54* 3′ UTR is expressed uniformly throughout the intestine [23]. However, a different expression pattern was observed in worms expressing *elo-2*^{prom}*::gfp::elo-2*$^{3'\ UTR}$, which showed little GFP expression in the int9 posterior intestinal cells relative to the neighboring int8 cells in most wild-type worms (Figures 5E and 5F). Loss of *mir-240/786* resulted in fewer worms that displayed this int9-specific repression of GFP (Figure 5G). For 3/5 transgenic lines, this pattern of reduced GFP expression in int9 posterior cells is significantly altered in *mir-240/786* mutant worms.

Deletion of the putative miR-786-binding site from the *elo-2* 3′ UTR resulted in weaker repression of GFP levels in the posterior intestine. Fewer worms expressing *elo-2*^{prom}*::gfp::elo-2*$^{3'\ UTRmut}$ showed low GFP expression in int9 relative to int8. No difference was observed between wild-type and *mir-240/786* mutants for 5/5 transgenic lines (Figure 5G). These data indicate that *elo-2* repression in int9 posterior cells requires the miR-786 binding site in the *elo-2* 3′ UTR and that *elo-2* is likely a direct target of miR-786 in the int9 posterior cells.

Knockdown of *elo-2* results in elevated levels of palmitate, which is sufficient to cause short defecation cycles in wild-type worms [23]. Therefore, we tested the hypothesis that the long arrhythmic defecation cycles in *mir-240/786* result from reduced palmitate levels caused by elevated *elo-2* activity. To test this, wild-type and *mir-240/786* worms were

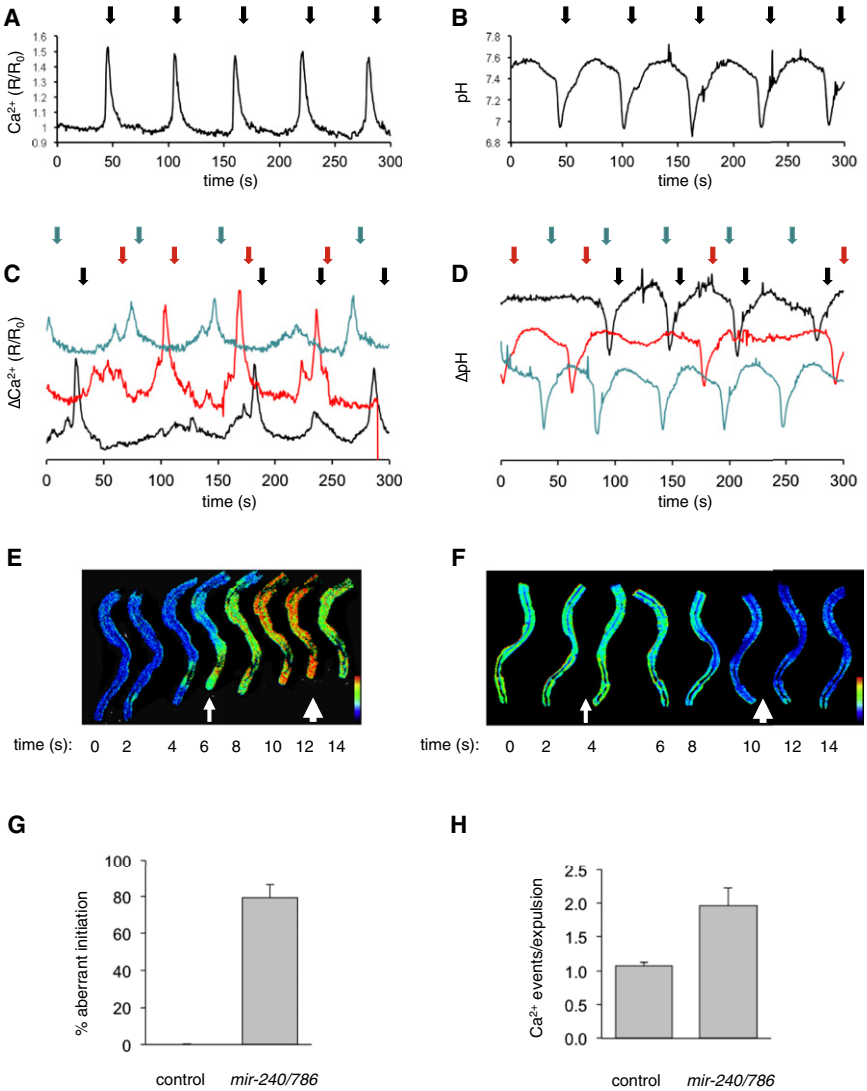

Figure 4. *mir-240/786* Spatially Constrains Calcium-Wave Initiation

Calcium was measured using dynamic imaging of live transgenic *C. elegans* expressing the dual emission fluorescent FRET-based calcium sensor D3cpV in the intestine, while pH was measured using fluorescent imaging of worms expressing the dual excitation pH biosensor pHluorin.

(A) A representative trace of oscillations in average intestinal calcium (R/R_0) in a congenic wild-type control worm.

(B) Representative intestinal pH oscillations in a congenic wild-type control worm.

(C) Three intestinal calcium traces from *mir-240/786* mutant worms, with the y axis scaled to wild-type and the individual traces offset from each other for clarity.

(D) Representative pH oscillations in *mir-240/786* mutants, as above. For the graphs shown in (A)–(D), the execution of the DMP is noted by block arrows color coded to the corresponding traces, located above the graph.

(E) An intestinal calcium heat map (red = elevated) illustrates ectopic calcium signals in *mir-240/786* mutants. In this representative case, a calcium signal arising in the cells proximal to the posterior intestine propagates in reverse and triggers a minor contraction of the posterior body-wall muscles (small arrow). This is followed shortly thereafter by a more robust increase in calcium, a second contraction, a calcium wave propagating in the forward direction, and execution of the full DMP (large arrow).

(F) A representative intestinal pH heat map (blue = acidic) where a weak pBoc (small arrow) is shown occurring in the absence of overt acidification, followed shortly thereafter by robust acidification and full DMP (large arrow).

(G) The supremacy of the posterior cell as pacemaker was quantified in control and mutant worms by assessing the initial site of calcium signaling that ultimately resulted in execution of the DMP. Calcium waves that initiated in the posterior and anterior cells nearly simultaneously were classified as normal. Signals arising elsewhere or in the anterior intestine alone were classified as aberrant.

(H) The number of calcium signaling events ($\sim R/R_0 > 1.1$) per expulsion step was determined using fluorescent imaging (for both G and H, 300 s imaging per worm, n = 8 for wild-type controls; n = 10 for *mir-240/786* mutants).

grown on plates supplemented with palmitate. Palmitate supplementation was sufficient to suppress the long arrhythmic defecation cycles in *mir-240/786* mutant worms, though wild-type worms did not show shorter defecation cycles in these experiments (Figure 5H). These data suggest that the *mir-240/786* defecation defects results from reduced palmitate levels in the posterior intestine, possibly by altering protein palmitoylation of regulatory membrane proteins or the lipid composition of cell membranes (Figure 5I).

Discussion

Defecation in wild-type worms is a stereotypical rhythmic behavior with a cycle period of ~50 s [25]. While calcium signaling in the intestine is central for this periodicity, the pacemaker mechanism that spatially constrains calcium-wave initiation is not understood. In this work, we have identified a miRNA cluster, *mir-240/786*, that is expressed in the posteriormost intestinal cells and is required for the rhythmic initiation of forward calcium waves. Our genetic and calcium imaging data indicate that *mir-240/786* functions upstream of IP_3-receptor activity to regulate calcium oscillations through the regulation of *elo-2*. Rescue experiments showed that *mir-786*, but not *mir-240*, is necessary for normal defecation cycling. miR-786 may function to either amplify the pacemaker signal that triggers calcium elevation or, alternatively, lower the threshold for calcium elevation in response to the pacemaker signal. Hence, by virtue of its expression pattern, *mir-786* can contribute to establishing or maintaining the supremacy of the posterior intestinal cells as the defecation pacemaker through the repression of *elo-2* and subsequent regulation of fatty-acid composition in the posterior intestine.

mir-240/786 mutants have defects in calcium elevation and wave initiation in the posterior intestine. In wild-type worms, calcium waves are initiated rhythmically in the posterior intestine. In contrast, in *mir-240/786* mutant worms, sites of calcium-wave initiation appear to be stochastic, with only ~20% of calcium waves initiating from the posterior intestine.

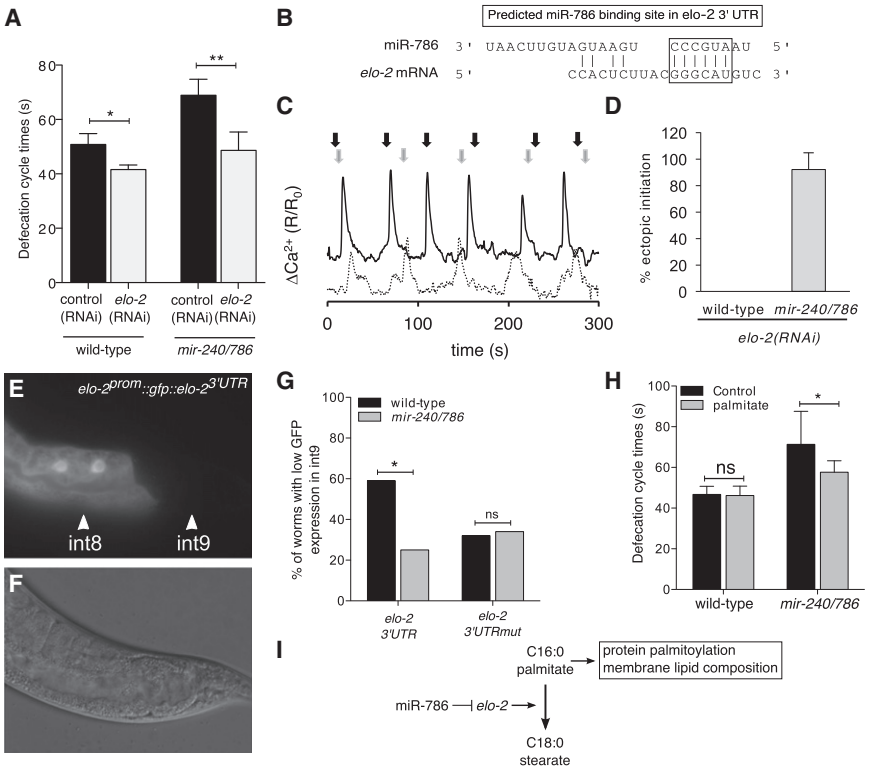

Figure 5. *elo-2* Is Likely a Direct Target of miR-786

(A) Knockdown of *elo-2* results in shorter defecation cycles in wild-type and *mir-240/786* worms. *p < 0.05, **p < 0.01. One-way ANOVA and Tukey's test. ns, not statistically significant; p > 0.05.

(B) Sequence of a putative miR-786 binding site within the *elo-2* 3′ UTR. The miR-786 alignment with the *elo-2* 3′ UTR is adapted from the mirWIP database [28].

(C) Representative traces of intestinal calcium oscillations in a *mir-240/786;elo-2(RNAi)* mutant worm (black) and a control *elo-2(RNAi)* worm (dashed). The traces have been offset from each other for clarity. The execution of the defecation motor program is noted by block arrows color coded to the corresponding traces.

(D) The supremacy of the posterior cell as pacemaker was quantified by assessing the initial site of calcium signaling that ultimately resulted in execution of the defecation motor program. Calcium waves that initiated in the posterior and anterior cells nearly simultaneously were classified as normal. Signals arising elsewhere or in the anterior intestine alone were classified as ectopic.

(E and F) Representative fluorescent micrograph (E) with corresponding differential interference contrast microscopy image (F) of the posterior intestine of a wild-type worm expressing low *elo-2*^{prom}*::gfp::elo-2*$^{3'\ UTR}$ transgene expression in int9 posterior intestinal cells.

(G) Worms were categorized based on the relative GFP expression level between int9 and their neighboring int8 cells. The percentage of worms that displayed low GFP expression in int9 relative to int8 was compared in wild-type and *mir-240/786* mutants. Expression was observed from a transgene under the regulation of the *elo-2* 3′ UTR as well as the *elo-2* 3′ UTR in which the predicted miR-786-binding site was deleted (3′ UTRmut). *p < 0.01 by chi-square analysis. ns, not significant.

(H) Palmitate supplementation suppresses the long-defecation-cycle defects of *mir-240/786* mutants. *p < 0.01. Two-way ANOVA and Bonferroni's test.

(I) Model for miR-786 function. Our data suggest that miR-786 repression of *elo-2* may regulate protein palmitoylation or membrane lipid composition to control calcium signaling in the intestine.

Similar ectopic calcium waves occur in *inx-16* mutants, which lack a pannexin gap junction protein [18], and *egl-8* mutants, which lack PLCβ activity [19]. It is likely that *inx-16* functions to maintain the supremacy of the posterior intestine by facilitating the forward propagation of calcium waves from the posterior intestine. The PLCβ protein, EGL-8, is enriched at points of cell-cell contact in the posterior intestine [32, 33] and may act to amplify and propagate forward calcium waves.

The observed defects in calcium oscillations and wave initiation can account for the defecation defects in *mir-240/786* mutants. First, *mir-240/786* mutants display arrhythmic posterior body contractions that correspond to the arrhythmic calcium oscillations. Second, we observed a biphasic execution of the posterior body contraction, with a weak partial contraction that immediately precedes a full contraction. This likely reflects minor calcium events that occur prior to a high-magnitude calcium release, which is sufficient to trigger robust acidification and a full posterior body contraction. In contrast, weak contractions were associated with slight pseudocoelomic acidification. Third, *mir-240/786* mutants had weak posterior contractions in the middle of defecation cycles, which are also likely due to the observed low-magnitude calcium events that fail to trigger robust acidification and a full contraction. Finally, we observed posterior body contractions that were not followed by an expulsion, which may result from calcium events in posterior cells that fail to propagate a forward calcium wave.

Our data suggest that posterior cells in *mir-240/786* mutants have reduced ability to either generate or respond to the pacemaker signal for calcium release, relative to wild-type worms. While we cannot strictly rule out a developmental effect of mir-240/786 on intestinal physiology, it appears more likely that the miRNA participates in the oscillatory calcium-signaling process. The pacemaker signal that initiates calcium release is unknown but may be calcium itself or IP_3 [14]. While miR-786 is necessary to establish or maintain the supremacy of the posterior intestine in the initiation of calcium waves and control of defecation cycling, it is likely not the only regulator that acts to ensure the supremacy of the posterior intestine. Rhythmic defecation and calcium wave initiation from the posterior intestine is observed in the absence of *mir-240/786* when the activity of the IP_3 receptor is elevated, through a gain-of-function mutation. This suggests that additional regulatory factors in the posterior intestine function downstream of IP_3-receptor-dependent calcium release to maintain the rhythmicity of defecation cycling. One such regulator may be EGL-8, which is localized in the posterior intestine and is required to ensure the rhythmic initiation of calcium waves from the posterior intestine [19].

miR-786 regulates defecation in part through the repression of *elo-2* in the posteriormost intestinal cells. *elo-2* is transcribed uniformly throughout the intestine [23]. Our data indicate that *elo-2* is repressed by miR-786 in the posterior intestine, which is predicted to result in lower ELO-2 protein

levels in int9 relative to neighboring cells. Our data indicate that miR-786 directly represses *elo-2* through the single predicted binding site in the *elo-2* 3′ UTR. Because some repression of *gfp* expression is observed in the absence of miR-786 and in the absence of the miR-786-binding site, it is likely that additional miRNAs or proteins function to regulate *elo-2* levels in the posterior intestine. A single binding site is expected to mediate modest repression [20], though the extent of repression depends upon the relative levels of miR-786 and *elo-2* mRNA [34]. Our expression analysis of reporter transgenes is consistent with a modest level of repression by miR-786. It remains possible that miR-786 functions to regulate additional targets that were not tested in this study.

miR-786 repression of *elo-2* is expected to alter the fatty-acid composition in the posteriormost intestinal cells. Reduced *elo-2* activity results in significantly elevated palmitate levels [23]. Interestingly, palmitate supplementation is sufficient to cause faster defecation cycles in wild-type worms [23] and to suppress the long arrhythmic defecation cycles in *mir-240/786* mutant worms. Therefore, miR-786 repression of *elo-2* activity in the posterior intestine may promote higher palmitate levels, which may enhance palmitoylation of key regulatory membrane proteins. Protein palmitoylation is a reversible modification and thus can provide dynamic regulation of the localization and activity of membrane proteins, including ion channels [35, 36]. Enhanced palmitoylation in the posterior intestine may sensitize these cells to promote faster calcium oscillations relative to the neighboring cells in the intestine.

One model to account for the intrinsic oscillating activity of calcium release involves the periodic entry of extracellular calcium. A small amount of calcium entry may be sufficient to either activate ITR-1 directly or to activate PLCγ activity, which produces IP_3 and triggers calcium release from the ER. Activation of PLCγ also lowers PIP_2 levels, which relieves the inhibition of TRPM calcium channels, GON-2/GTL-1, at the plasma membrane [13, 14]. Calcium flux through both GON-2/GTL-1 TRPM channels and ITR-1 IP_3-receptor channels contributes to robust cytoplasmic calcium elevation [9–11, 13]. We speculate that miR-786 repression of ELO-2 levels in the posterior intestinal cells establishes differences in the levels of fatty acids, such as palmitate, that could modulate the activity of membrane proteins, which control calcium signaling. Candidate membrane proteins that may be regulated by palmitoylation include the GON-2/GTL-1 TRPM channels, the ITR-1 IP_3 receptor, and KQT-2/3 KCNQ potassium channels, which contain putative palmitoylation sites identified using the CSS-Palm 3.0 prediction algorithm [37]. Increased palmitoylation may lower the threshold for calcium elevation in the int9 posteriormost cells and thereby ensure faster calcium oscillations and reliable calcium-wave initiation from these cells. Alternatively, differences in lipid composition of the membranes in the posterior intestine may promote targeting regulatory proteins to the plasma membrane that may act to regulate calcium release.

Experimental Procedures

General Procedures

C. elegans strains were maintained at 20°C on *Escherichia coli* strain AMA1004 under standard conditions. Strains used are listed in Table S3. The Supplemental Experimental Procedures contain detailed information on strain and plasmid construction, microscopy, calcium and pH imaging, RNAi, qPCR, and fatty-acid supplements.

Defecation Assays

For wild-type and mutant strains, young adult worms (within 24 hr of the L4 molt) were scored at room temperature. The time interval between consecutive pBoc contractions was scored for 11 consecutive pBoc contractions. For each strain, 6–10 worms were analyzed. Statistical analysis was performed using ANOVA followed by Tukey's multiple comparison tests using Prism 5.0 (GraphPad software).

Supplemental Information

Supplemental Information includes three figures, three tables, Supplemental Experimental Procedures, and two movies and can be found with this article online at http://dx.doi.org/10.1016/j.cub.2012.09.047.

Acknowledgments

Some strains used in this study were obtained from the Caenorhabditis Genetics Center (CGC), which is supported by a grant from the National Institutes of Health (NIH, National Center for Research Resources). This work was supported by NIH grant R15-GM084451 to A.L.A., NSF grant IOS0919848 to K.N., and an NSF-RUI 0842830 grant to M.A.P.

Received: May 30, 2012
Revised: August 30, 2012
Accepted: September 26, 2012
Published: November 8, 2012

References

1. Baruscotti, M., Barbuti, A., and Bucchi, A. (2010). The cardiac pacemaker current. J. Mol. Cell. Cardiol. *48*, 55–64.
2. Berridge, M.J. (2008). Smooth muscle cell calcium activation mechanisms. J. Physiol. *586*, 5047–5061.
3. Irisawa, H., Brown, H.F., and Giles, W. (1993). Cardiac pacemaking in the sinoatrial node. Physiol. Rev. *73*, 197–227.
4. Sanders, K.M., Koh, S.D., and Ward, S.M. (2006). Interstitial cells of cajal as pacemakers in the gastrointestinal tract. Annu. Rev. Physiol. *68*, 307–343.
5. Avery, L., and Thomas, J.H. (1997). Feeding and defecation. In *C. elegans* II, D.L. Riddle, T. Blumenthal, B.J. Meyer, and J.R. Priess, eds. (Cold Spring Harbor, NY: Cold Spring Harbor Laboratory Press), pp. 679–716.
6. McCarter, J., Bartlett, B., Dang, T., and Schedl, T. (1999). On the control of oocyte meiotic maturation and ovulation in *Caenorhabditis elegans*. Dev. Biol. *205*, 111–128.
7. Thomas, J.H. (1990). Genetic analysis of defecation in *Caenorhabditis elegans*. Genetics *124*, 855–872.
8. Allman, E., Thyagarajan, B., and Nehrke, K. (2012). The inositol 1, 4, 5-trisphosphate receptor in *C. elegans*. WIREs Membr. Transp. Signal. *1*, 321–328.
9. Dal Santo, P., Logan, M.A., Chisholm, A.D., and Jorgensen, E.M. (1999). The inositol trisphosphate receptor regulates a 50-second behavioral rhythm in *C. elegans*. Cell *98*, 757–767.
10. Espelt, M.V., Estevez, A.Y., Yin, X., and Strange, K. (2005). Oscillatory Ca^{2+} signaling in the isolated *Caenorhabditis elegans* intestine: role of the inositol-1,4,5-trisphosphate receptor and phospholipases C beta and gamma. J. Gen. Physiol. *126*, 379–392.
11. Teramoto, T., and Iwasaki, K. (2006). Intestinal calcium waves coordinate a behavioral motor program in *C. elegans*. Cell Calcium *40*, 319–327.
12. Kwan, C.S., Vázquez-Manrique, R.P., Ly, S., Goyal, K., and Baylis, H.A. (2008). TRPM channels are required for rhythmicity in the ultradian defecation rhythm of *C. elegans*. BMC Physiol. *8*, 11.
13. Xing, J., Yan, X., Estevez, A., and Strange, K. (2008). Highly Ca2+-selective TRPM channels regulate IP_3-dependent oscillatory Ca2+ signaling in the *C. elegans* intestine. J. Gen. Physiol. *131*, 245–255.
14. Xing, J., and Strange, K. (2010). Phosphatidylinositol 4,5-bisphosphate and loss of PLCgamma activity inhibit TRPM channels required for oscillatory Ca2+ signaling. Am. J. Physiol. Cell Physiol. *298*, C274–C282.
15. Beg, A.A., Ernstrom, G.G., Nix, P., Davis, M.W., and Jorgensen, E.M. (2008). Protons act as a transmitter for muscle contraction in *C. elegans*. Cell *132*, 149–160.

16. Pfeiffer, J., Johnson, D., and Nehrke, K. (2008). Oscillatory transepithelial H(+) flux regulates a rhythmic behavior in *C. elegans*. Curr. Biol. *18*, 297–302.
17. McGhee, J.D. (2007). The C. elegans intestine. WormBook, 1–36.
18. Peters, M.A., Teramoto, T., White, J.Q., Iwasaki, K., and Jorgensen, E.M. (2007). A calcium wave mediated by gap junctions coordinates a rhythmic behavior in *C. elegans*. Curr. Biol. *17*, 1601–1608.
19. Nehrke, K., Denton, J., and Mowrey, W. (2008). Intestinal Ca2+ wave dynamics in freely moving C. elegans coordinate execution of a rhythmic motor program. Am. J. Physiol. Cell Physiol. *294*, C333–C344.
20. Bartel, D.P. (2009). MicroRNAs: target recognition and regulatory functions. Cell *136*, 215–233.
21. Stefani, G., and Slack, F.J. (2008). Small non-coding RNAs in animal development. Nat. Rev. Mol. Cell Biol. *9*, 219–230.
22. Miska, E.A., Alvarez-Saavedra, E., Abbott, A.L., Lau, N.C., Hellman, A.B., McGonagle, S.M., Bartel, D.P., Ambros, V.R., and Horvitz, H.R. (2007). Most *Caenorhabditis elegans* microRNAs are individually not essential for development or viability. PLoS Genet. *3*, e215.
23. Kniazeva, M., Sieber, M., McCauley, S., Zhang, K., Watts, J.L., and Han, M. (2003). Suppression of the ELO-2 FA elongation activity results in alterations of the fatty acid composition and multiple physiological defects, including abnormal ultradian rhythms, in *Caenorhabditis elegans*. Genetics *163*, 159–169.
24. Martinez, N.J., Ow, M.C., Reece-Hoyes, J.S., Barrasa, M.I., Ambros, V.R., and Walhout, A.J. (2008). Genome-scale spatiotemporal analysis of *Caenorhabditis elegans* microRNA promoter activity. Genome Res. *18*, 2005–2015.
25. Branicky, R., and Hekimi, S. (2006). What keeps *C. elegans* regular: the genetics of defecation. Trends Genet. *22*, 571–579.
26. Walker, D.S., Gower, N.J.D., Ly, S., Bradley, G.L., and Baylis, H.A. (2002). Regulated disruption of inositol 1,4,5-trisphosphate signaling in *Caenorhabditis elegans* reveals new functions in feeding and embryogenesis. Mol. Biol. Cell *13*, 1329–1337.
27. Palmer, A.E., Giacomello, M., Kortemme, T., Hires, S.A., Lev-Ram, V., Baker, D., and Tsien, R.Y. (2006). Ca^{2+} indicators based on computationally redesigned calmodulin-peptide pairs. Chem. Biol. *13*, 521–530.
28. Hammell, M., Long, D., Zhang, L., Lee, A., Carmack, C.S., Han, M., Ding, Y., and Ambros, V. (2008). mirWIP: microRNA target prediction based on microRNA-containing ribonucleoprotein-enriched transcripts. Nat. Methods *5*, 813–819.
29. Kertesz, M., Iovino, N., Unnerstall, U., Gaul, U., and Segal, E. (2007). The role of site accessibility in microRNA target recognition. Nat. Genet. *39*, 1278–1284.
30. Jan, C.H., Friedman, R.C., Ruby, J.G., and Bartel, D.P. (2011). Formation, regulation and evolution of Caenorhabditis elegans 3′UTRs. Nature *469*, 97–101.
31. Lewis, B.P., Burge, C.B., and Bartel, D.P. (2005). Conserved seed pairing, often flanked by adenosines, indicates that thousands of human genes are microRNA targets. Cell *120*, 15–20.
32. Lackner, M.R., Nurrish, S.J., and Kaplan, J.M. (1999). Facilitation of synaptic transmission by EGL-30 Gqalpha and EGL-8 PLCbeta: DAG binding to UNC-13 is required to stimulate acetylcholine release. Neuron *24*, 335–346.
33. Miller, K.G., Emerson, M.D., and Rand, J.B. (1999). Goalpha and diacylglycerol kinase negatively regulate the Gqalpha pathway in *C. elegans*. Neuron *24*, 323–333.
34. Mukherji, S., Ebert, M.S., Zheng, G.X.Y., Tsang, J.S., Sharp, P.A., and van Oudenaarden, A. (2011). MicroRNAs can generate thresholds in target gene expression. Nat. Genet. *43*, 854–859.
35. Shipston, M.J. (2011). Ion channel regulation by protein palmitoylation. J. Biol. Chem. *286*, 8709–8716.
36. Smotrys, J.E., and Linder, M.E. (2004). Palmitoylation of intracellular signaling proteins: regulation and function. Annu. Rev. Biochem. *73*, 559–587.
37. Ren, J., Wen, L., Gao, X., Jin, C., Xue, Y., and Yao, X. (2008). CSS-Palm 2.0: an updated software for palmitoylation sites prediction. Protein Eng. Des. Sel. *21*, 639–644.